

Assimilation in the Unstable Subspace

Olivier Talagrand

Laboratoire de Météorologie Dynamique, École Normale Supérieure, Paris, France

Durham Symposium *Mathematics of Data Assimilation*

London Mathematical Society

Engineering and Physical Sciences Research Council

Durham, UK

8 August 2011

Trevisan *et al.*, 2010, Four-dimensional variational assimilation in the unstable subspace and the optimal subspace dimension, *Q. J. R. Meteorol. Soc.*, **136**, 487-496.

Related to

M. Ghil's presentation on Tuesday 2 August (extension from 3D to 4D)

D. McLaughlin's presentation on Thursday 4 (essentially the same results, but for 4DVar instead of EnKF).

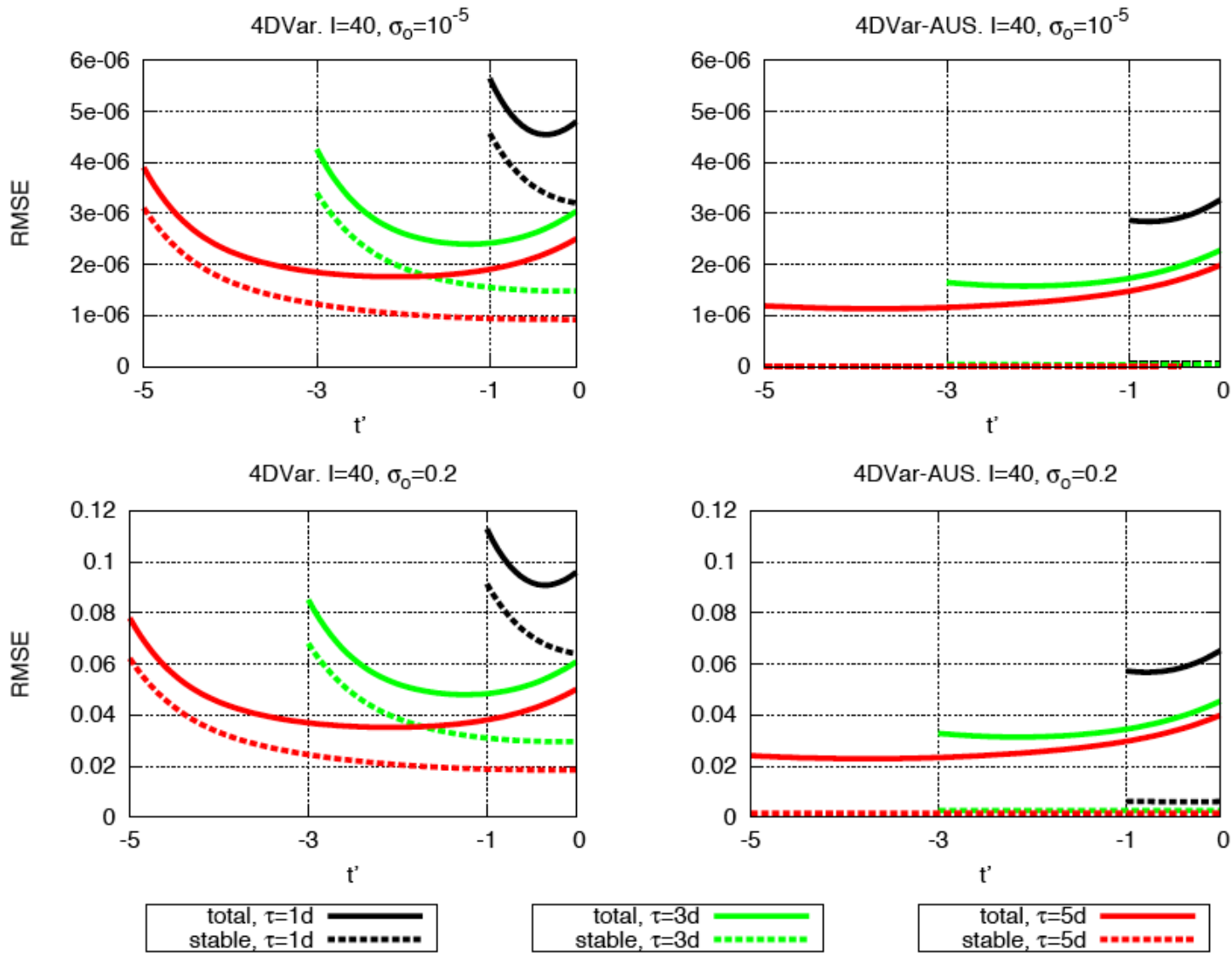
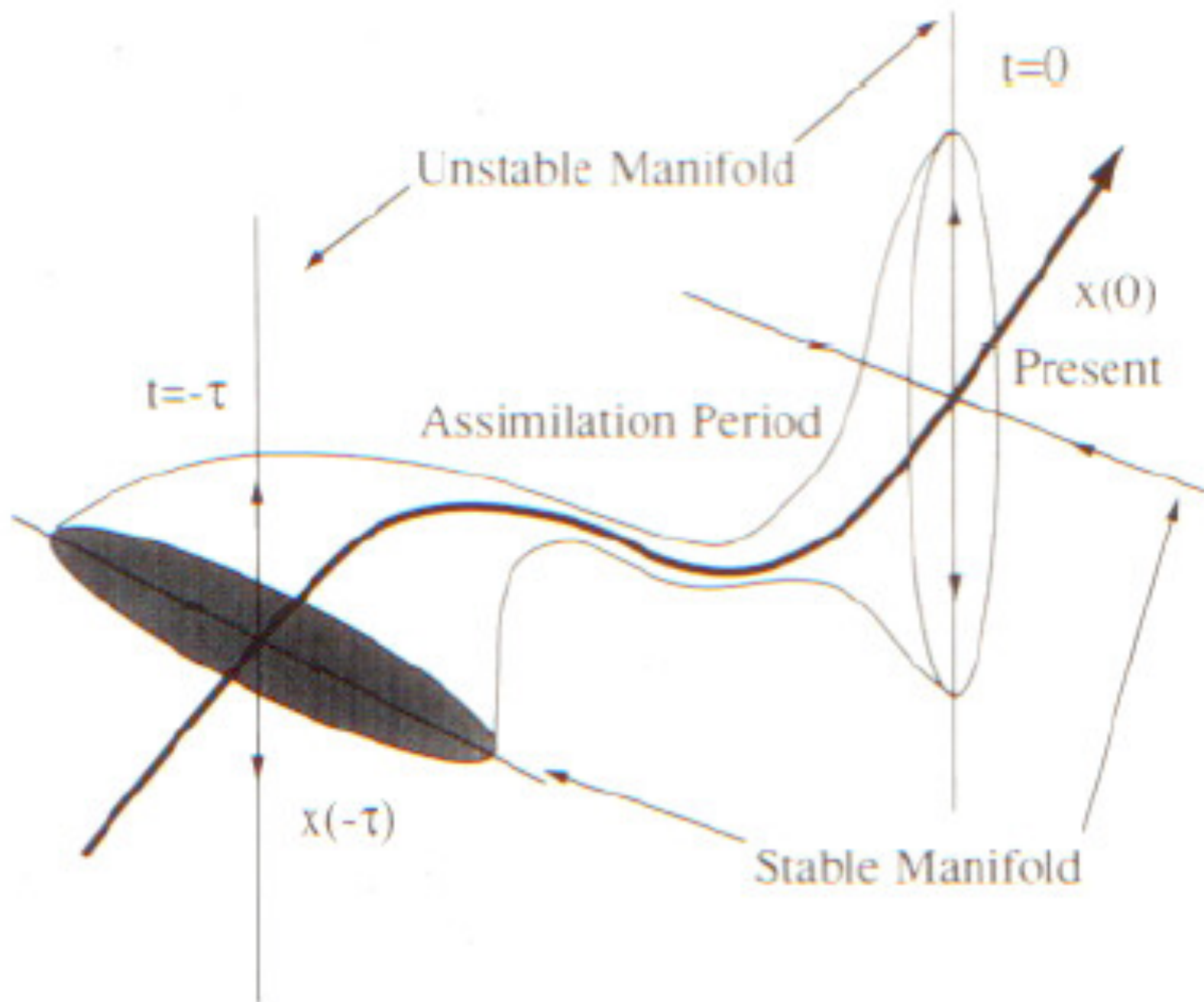


Figure 3. Time average RMS error within 1, 3, 5 days assimilation windows as a function of $t' = t - \tau$, with $\sigma_0 = .2, 10^{-5}$ for the model configuration $I = 40$. Left panel: 4DVar. Right panel: 4DVar-AUS with $N = 15$. Solid lines refer to total assimilation error, dashed lines refer to the error component in the stable subspace e_{16}, \dots, e_{40} .



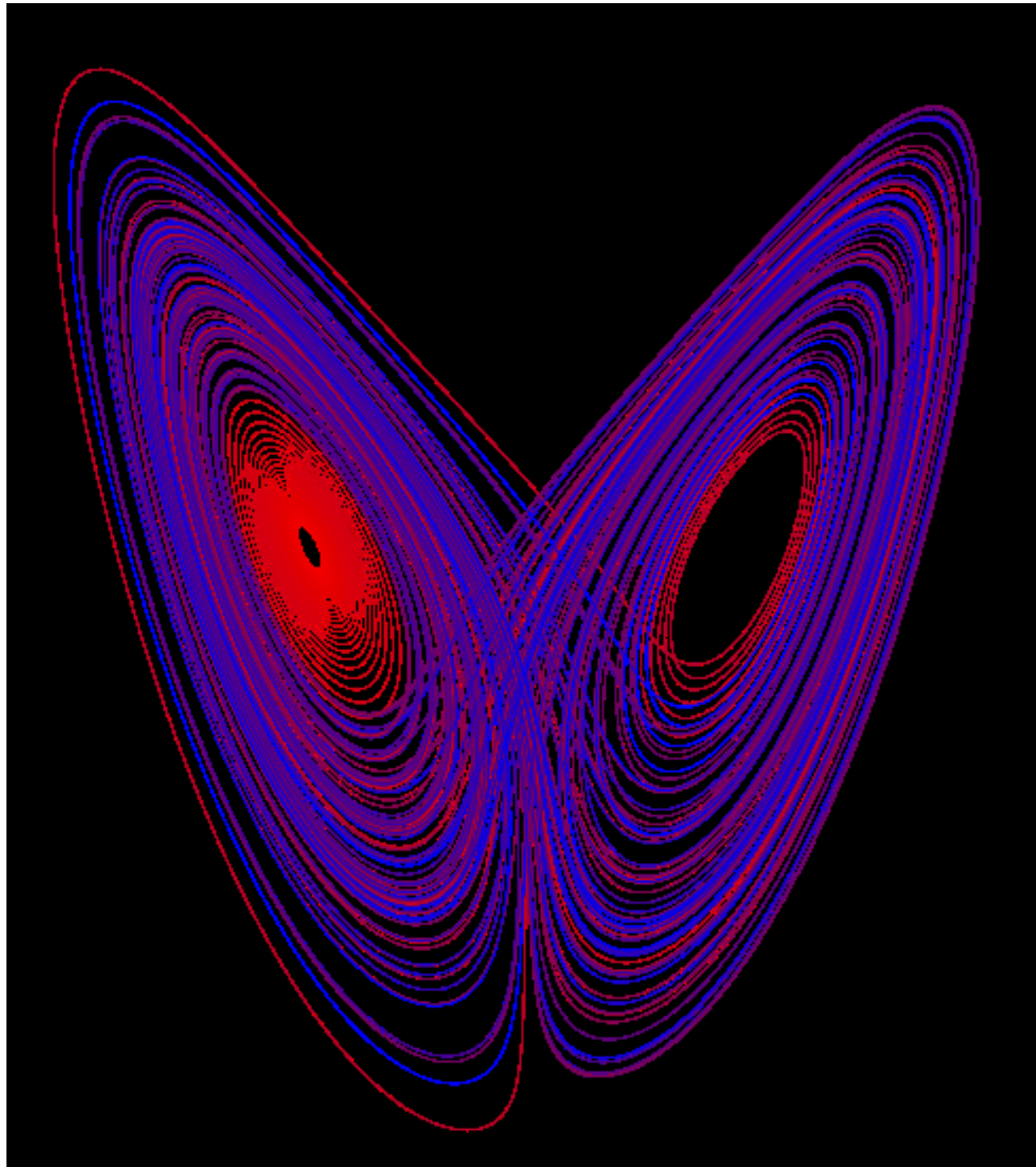
Lorenz (1963)

$$dx/dt = \sigma(y-x)$$

$$dy/dt = \rho x - y - xz$$

$$dz/dt = -\beta z + xy$$

with parameter values $\sigma = 10$, $\rho = 28$, $\beta = 8/3 \Rightarrow$ chaos



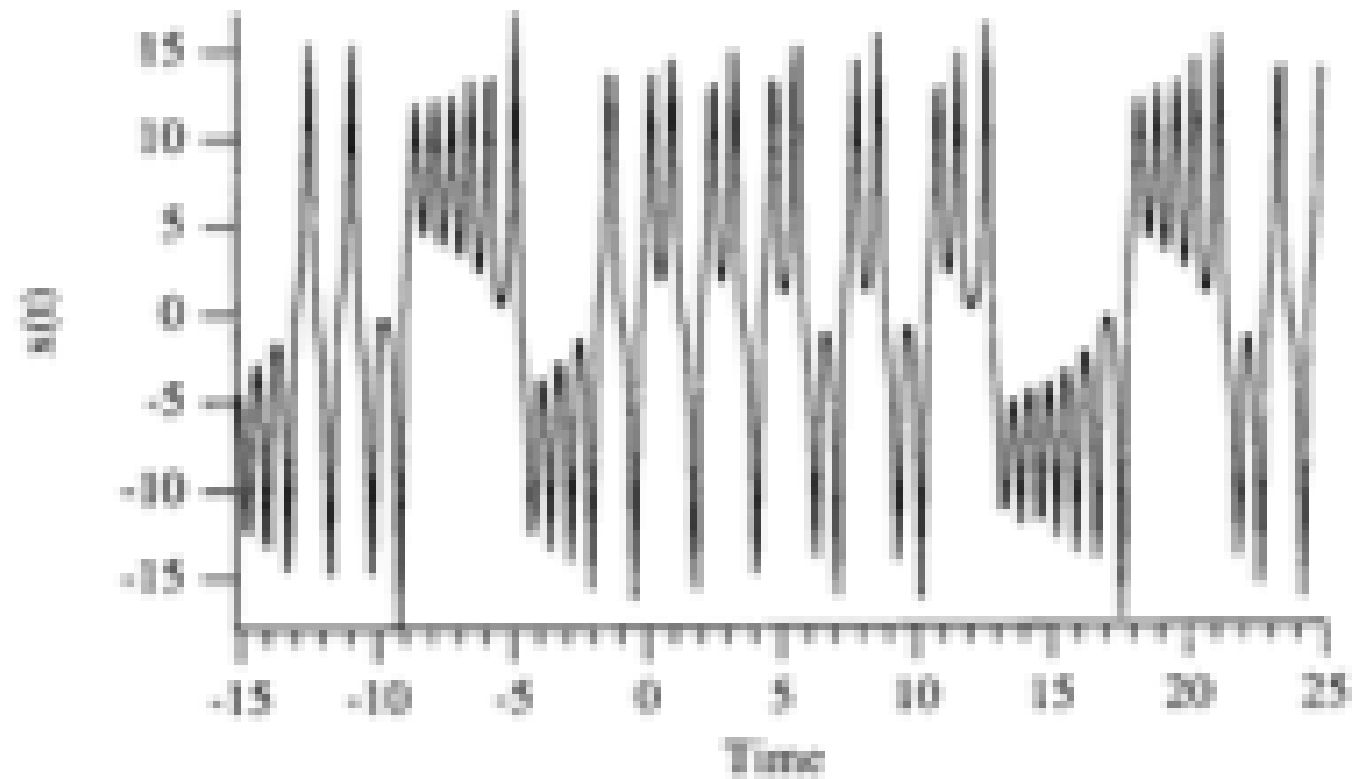


Fig. 2. Time variations, along the reference solution, of the variable $x(t)$ of the Lorenz system.

Pires *et al.*, *Tellus*, 1996 ; Lorenz system (1963)

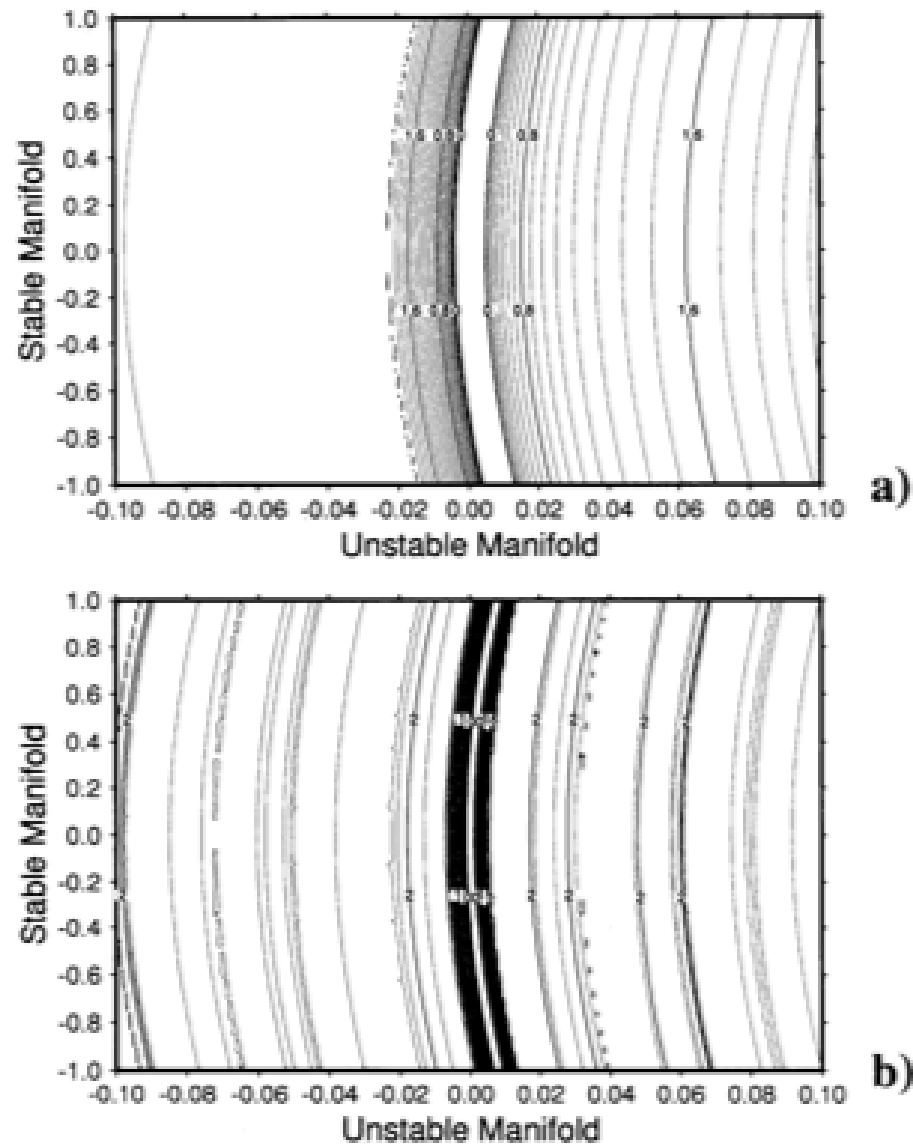


Fig. 3. Variations of the error-free forward cost-function $J_0(r, x)$ (Lorenz system) in the plane spanned by the stable and unstable directions, as determined from the tangent linear system (see text), and for $r = 6$ (panel (a)) and $r = 8$ (panel (b)) respectively. The metric has been distorted in order to make the stable and unstable manifolds orthogonal to each other in the figure. The scale on the contour lines is logarithmic (decimal logarithm). Contour interval: 0.1. For clarity, negative contours, which would be present only in the central "valley" directed along the stable manifold, have not been drawn.

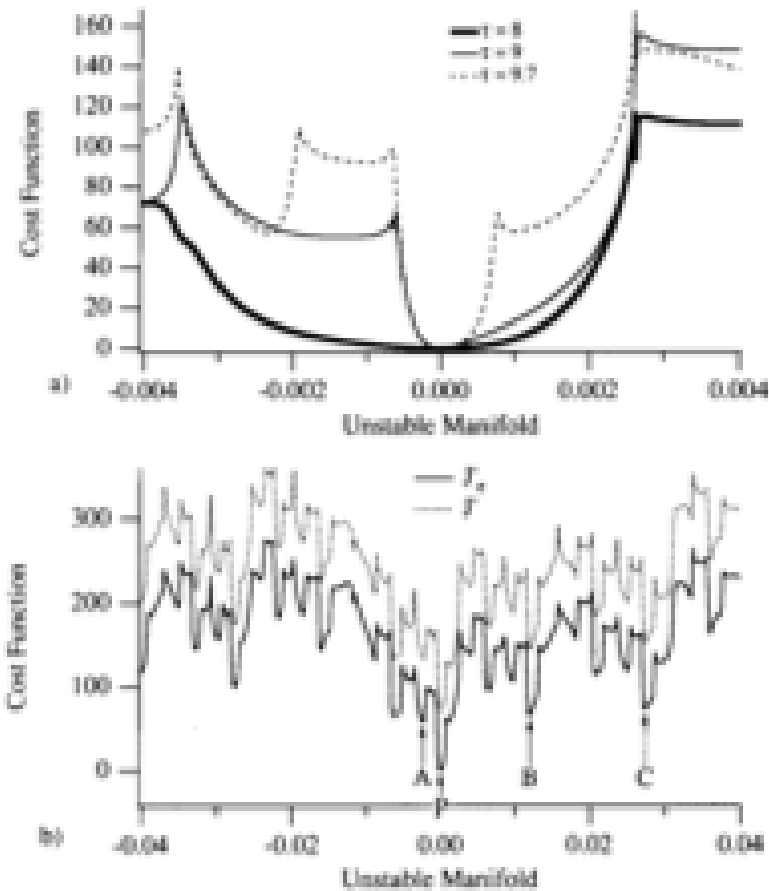


Fig. 4. Panel (a): Cross-section of the error-free forward cost-function $J_a^*(\tau, \xi, x)$ along the unstable manifold, for various values of τ . Panel (b). As in panel (a), for $\tau = 9.7$, and with a display interval ten times as large, respectively for the error-free forward cost-function $J_a^*(\tau, \xi, x)$ (solid curve) and for the error-contaminated cost-function $J_a(\tau, \xi, x)$ (dashed curve). In the latter case, the total variance of the observational noise is $E^2 = 75$.

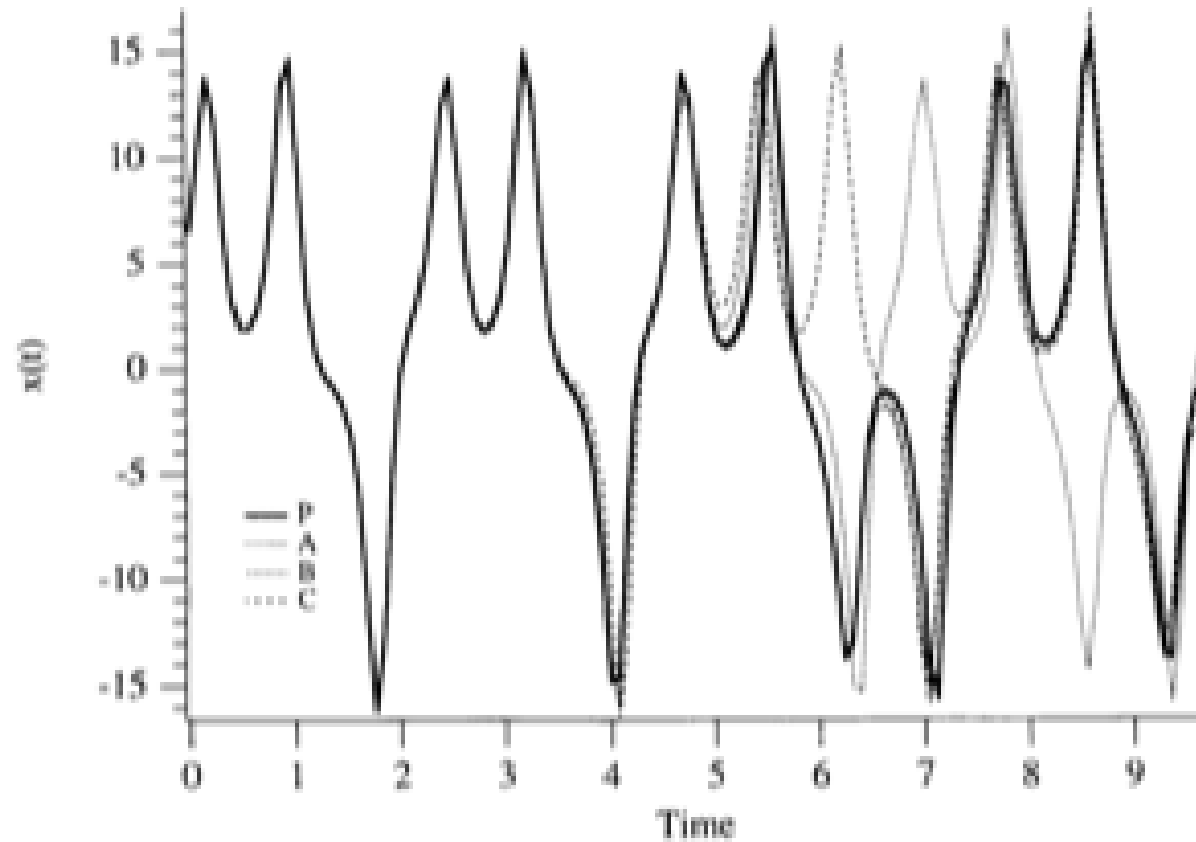


Fig. 5. Variations of the coordinate x along the orbits originating from the minima P , A , B , C (indicated in Fig. 4b) of the error-free cost-function.

Minima in the variations of objective function correspond to solutions that have bifurcated from the observed solution, and to different folds in state space.

Quasi-Static Variational Assimilation (QSVA). Increase progressively length of the assimilation window, starting each new assimilation from the result of the previous one. This should ensure, at least if observations are in a sense sufficiently dense in time, that current estimation of the system always lies in the basin of attraction of the absolute minimum of objective function.

One complete (Lorenz 63) state vector observed every $\delta t = 0.1$, with unbiased Gaussian white noise with unit covariance matrix in coordinates (x, y, z) .

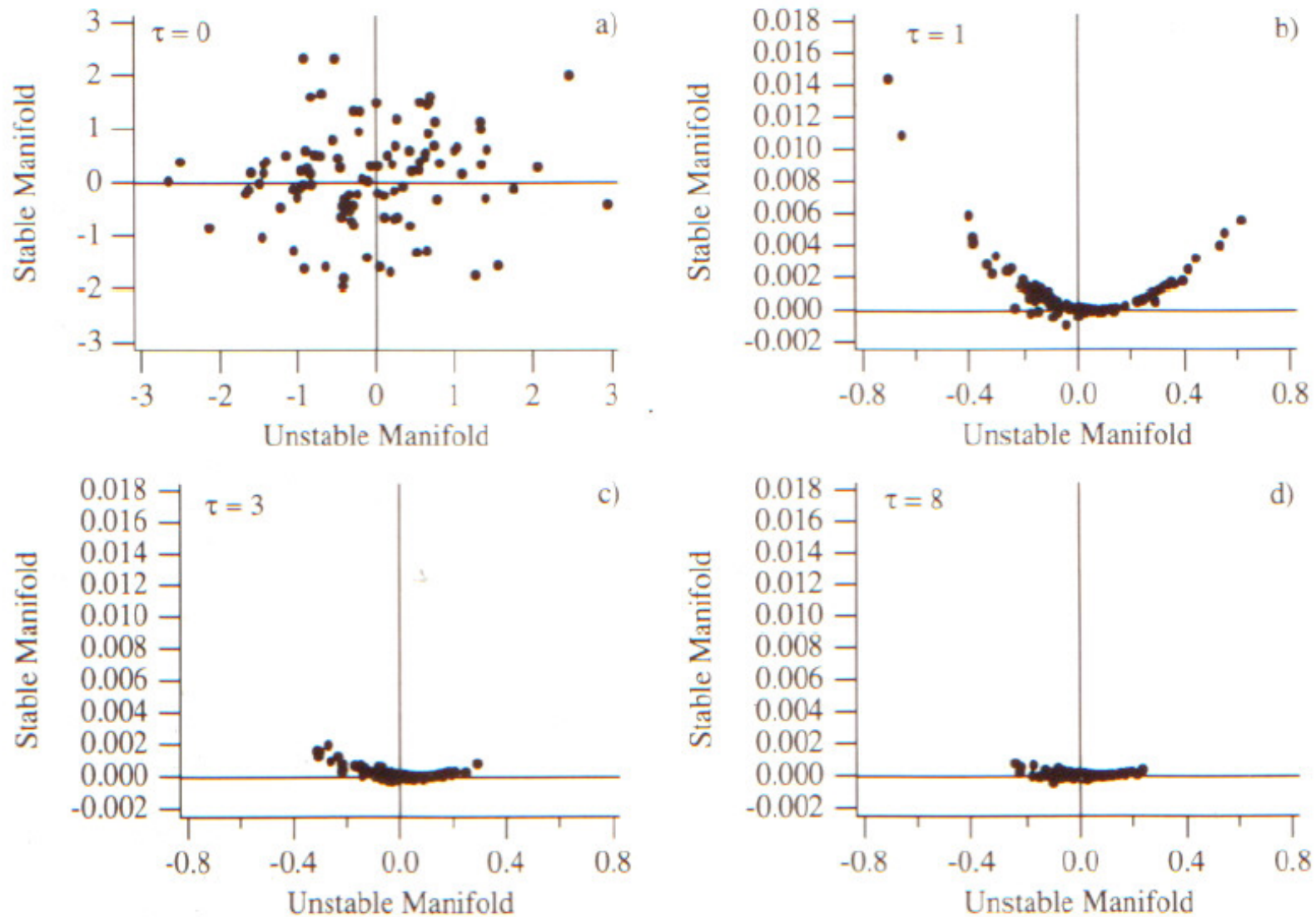


Fig. 7. Projection of the 100 minimizing solutions, at the end of the assimilation period, onto the plane spanned by the stable and unstable directions, defined as in Fig. 3. Values of τ are indicated on the panels. The projection is not an orthogonal projection, but a projection parallel to the local velocity vector $(dx/dt, dy/dt, dz/dt)$ (central manifold).

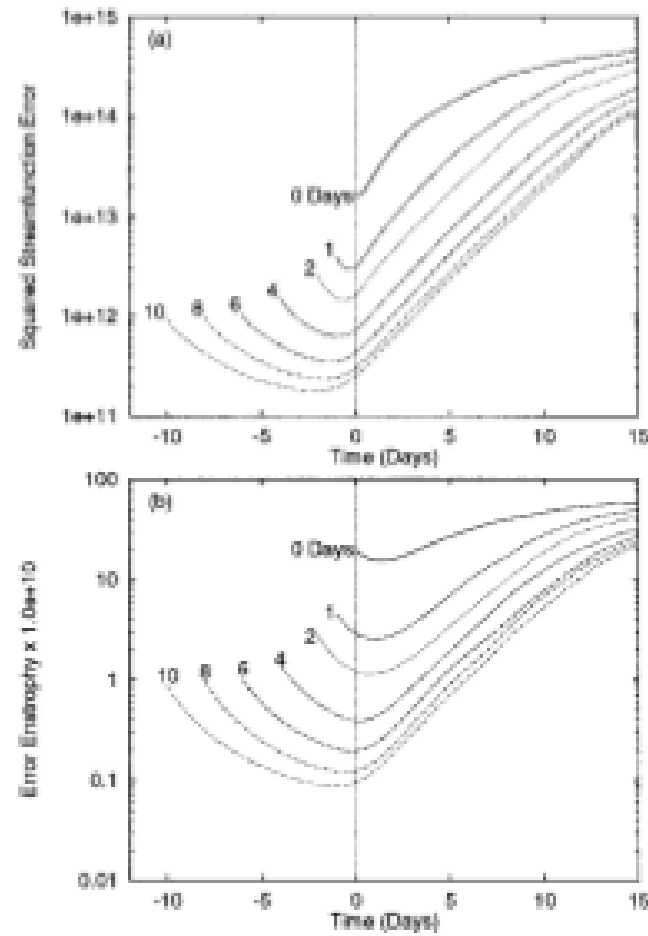


Fig. 5. Median values of the (a) streamfunction squared error, and (b) enstrophy error for the 200 forecast set as a function of forecast time and of the assimilation time T_a .

Swanson, Vautard and Pires, 1998, *Tellus*, **50A**, 369-390

Since, after an assimilation has been performed over a period of time, uncertainty is likely to be concentrated in modes that have been unstable, it might be useful for the next assimilation, and at least in terms of cost efficiency, to concentrate corrections on the background in those modes.

Actually, presence of residual noise in stable modes can be damageable for analysis and subsequent forecast.

Assimilation in the Unstable Subspace (AUS) (Carrassi *et al.*, 2007, 2008, for the case of 3D-Var, M. Ghil)

And also, as concerns Extended Kalman Filter

Trevisan, A., and L. Palatella, On the Kalman Filter error covariance collapse into the unstable subspace, *Nonlin. Processes Geophys.*, **18**, 243–250, 2011.

D. McLaughlin for Ensemble Kalman Filter

Four-dimensional variational assimilation in the unstable subspace
(4DVar-AUS)

Trevisan *et al.*, 2010, Four-dimensional variational assimilation in the unstable subspace and the optimal subspace dimension, *Q. J. R. Meteorol. Soc.*, **136**, 487-496.

4D-Var-AUS

Algorithmic implementation

Define N perturbations to the current state, and evolve them according to the tangent linear model, with periodic reorthonormalization in order to avoid collapse onto the dominant Lyapunov vector (same algorithm as for computation of Lyapunov exponents).

Cycle successive 4D-Var's, restricting at each cycle the modification to be made on the current state to the space spanned by the N perturbations emanating from the previous cycle (if N is the dimension of state space, that is identical with standard 4D-Var).

Experiments performed on the Lorenz (1996) model

$$\frac{d}{dt}x_j = (x_{j+1} - x_{j-2})x_{j-1} - x_j + F$$

with $j = 1, \dots, I$.

with value $F = 8$, which gives rise to chaos.

Three values of I have been used, namely $I = 40, 60, 80$, which correspond to respectively $N^+ = 13, 19$ and 26 positive Lyapunov exponents.

In all three cases, the largest Lyapunov exponent corresponds to a doubling time of about 2 days (with 1 'day' = 1/5 model time unit).

Identical twin experiments (perfect model)

‘Observing system’ defined as in Fertig *et al.* (*Tellus*, 2007):

At each observation time, one observation every four grid points (observation points shifted by one grid point at each observation time).

Observation frequency : 1.5 hour

Random gaussian observation errors with expectation 0 and standard deviation $\sigma_0 = 0.2$ (‘climatological’ standard deviation 5.1).

Sequences of variational assimilations have been cycled over windows with length $\tau = 1, \dots, 5$ days. Results are averaged over 5000 successive windows.

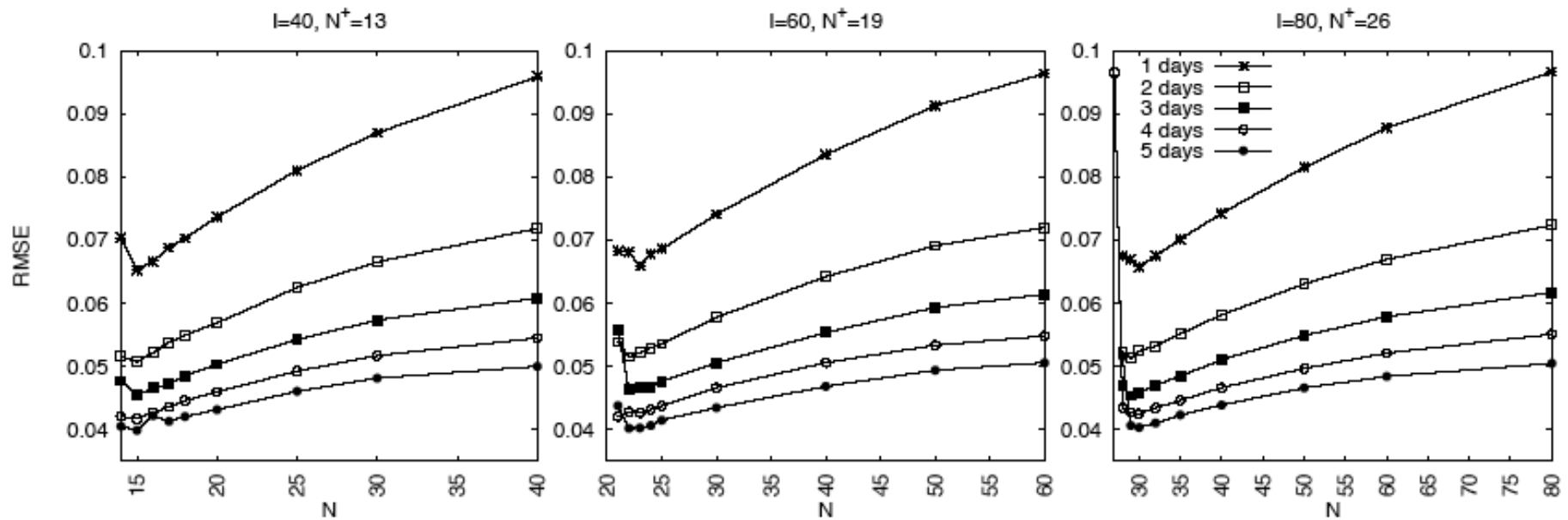


Figure 1. Time average RMS analysis error at $t = \tau$ as a function of the subspace dimension N for three model configurations: $I=40, 60, 80$. Different curves in the same panel refer to different assimilation windows from 1 to 5 days. The observation error standard deviation is $\sigma_o = 0.2$.

No explicit background term (*i. e.*, with error covariance matrix) in objective function : information from past lies in the background to be updated, and in the N perturbations which define the subspace in which updating is to be made.

Best performance for N slightly above number N^+ of positive Lyapunov exponents.

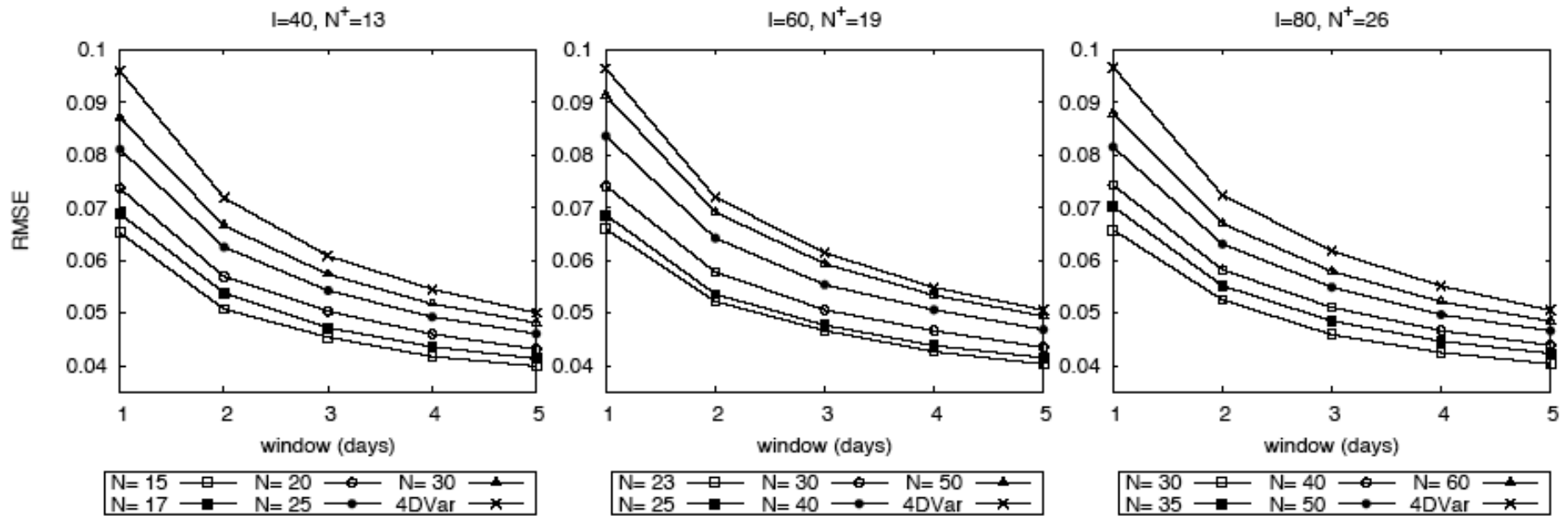


Figure 2. Time average RMS analysis error at $t = \tau$ as a function of the length of the assimilation window for three model configurations: $I=40, 60, 80$. Different curves in the same panel refer to a different subspace dimension N of 4DVar-AUS and to standard 4DVar. $\sigma_o = 0.2$.

Different curves are almost identical on all three panels. Relative improvement obtained by decreasing subspace dimension N to its optimal value is largest for smaller window length τ .

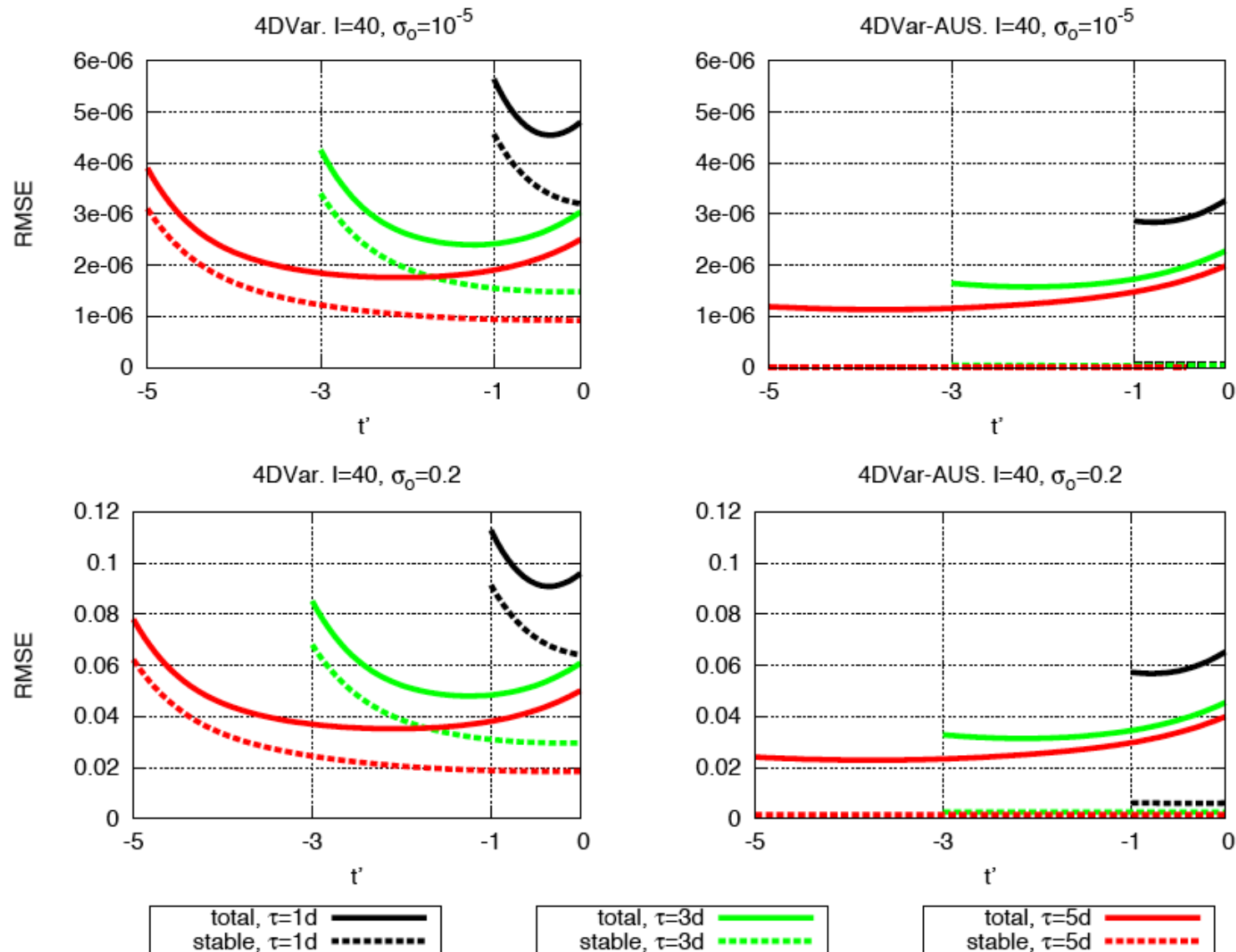


Figure 3. Time average RMS error within 1, 3, 5 days assimilation windows as a function of $t' = t - \tau$, with $\sigma_0 = .2, 10^{-5}$ for the model configuration $I = 40$. Left panel: 4DVar. Right panel: 4DVar-AUS with $N = 15$. Solid lines refer to total assimilation error, dashed lines refer to the error component in the stable subspace e_{16}, \dots, e_{40} .

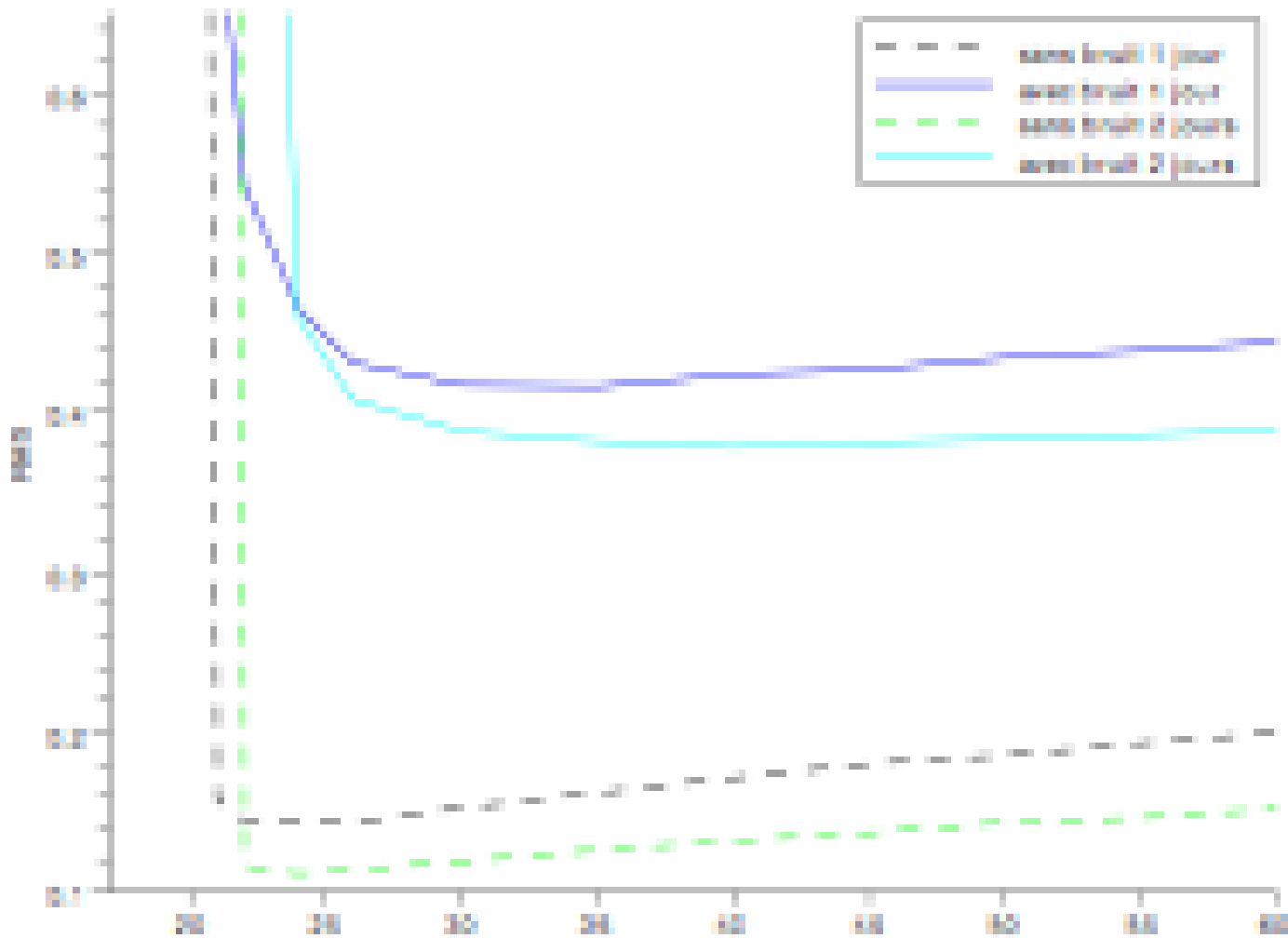
Experiments have been performed in which an explicit background term was present, the associated error covariance matrix having been obtained as the average of a sequence of full 4D-Var's.

The estimates are systematically improved, and more for full 4D-Var than for 4D-Var-AUS. But they remain qualitatively similar, with best performance for 4D-Var-AUS with N slightly above N^+ .

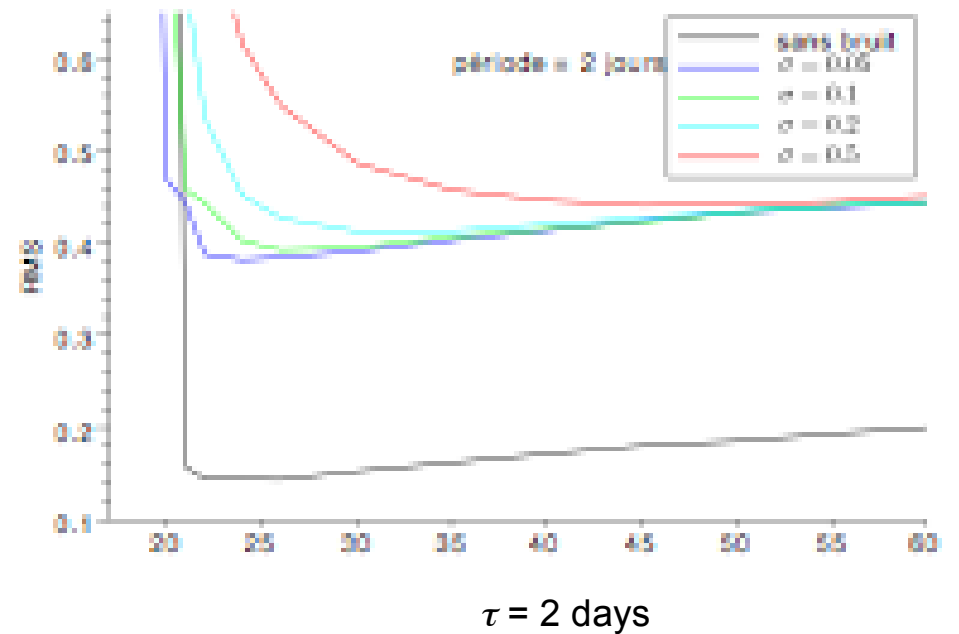
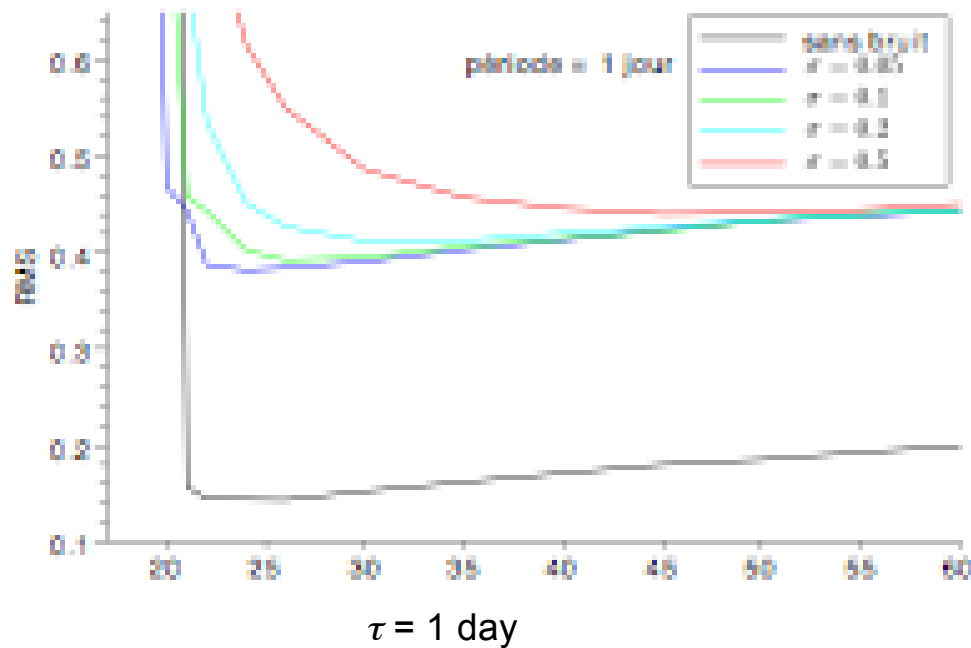
Minimum of objective function cannot be made smaller by reducing control space. Numerical tests show that minimum of objective function is smaller (by a few percent) for full 4D-Var than for 4D-Var-AUS. Full 4D-Var is closer to the noisy observations, but farther away from the truth. And tests also show that full 4D-Var performs best when observations are perfect (no noise).

Results show that, if all degrees of freedom that are available to the model are used, and if observations are noisy, the minimization process introduces components along the stable modes of the system, in which no error is present, in order to ensure a closer fit to the observations. This degrades the closeness of the fit to reality. The optimal choice is to restrict the assimilation to the unstable modes.

- Impact of model errors ?



Time averaged rms analysis error at the end τ of the assimilation window as a function of increment subspace dimension ($l = 60$, $N^+=19$). Lower curves : no model noise ($\tau = 1$ and 2 days). Upper curves : constant model noise ($\tau = 1$ and 2 days) (W. Ohayon and O. Pannekoucke, 2011).



Time averaged rms analysis error at the end τ of the assimilation window as a function of increment subspace dimension ($I = 60$, $N^+ = 19$), for different amplitudes of white model noise.

(W. Ohayon and O. Pannekoucke, 2011).

Conclusions

Error concentrates in unstable modes at the end of assimilation window. It must therefore be sufficient, at the beginning of new assimilation cycle, to introduce increments only in the subspace spanned by those unstable modes.

In the perfect model case, assimilation is most efficient when increments are introduced in a space with dimension slightly above the number of non-negative Lyapunov exponents.

In the case of imperfect model (and of strong constraint assimilation), preliminary results lead to similar conclusions, with larger optimal subspace dimension, and less well marked optimality. Further work necessary.

In agreement with theoretical and experimental results obtained for Kalman Filter assimilation (Trevisan and Palatella, McLaughlin).

Thanks !